geographies

MDPI

Article

The Importance of the Census of Anthropogenic Cavities in the Mitigation Geological Hazards: The Case of Grotte di Castro (Italy)

Francesco Gentili [1,*], Sergio Madonna [2] and Stefania Nisio [3]

[1] Department of Ecological and Biological Sciences, Tuscia University, Via San Camillo De Lellis Snc, 01100 Viterbo, Italy
[2] Department of Agriculture and Forest Sciences, Tuscia University, Via San Camillo De Lellis Snc, 01100 Viterbo, Italy; sermad@unitus.it
[3] Geological Survey of Italy, Italian Institute for Environmental Protection and Research (ISPRA), Via Vitaliano Brancati 60, 00144 Rome, Italy; stefania.nisio@isprambiente.it
* Correspondence: francesco.gentili@unitus.it

Abstract: The municipality of Grotte di Castro (Lazio Region, Italy) has, for some time, been the subject of various studies concerning the census of artificial cavities. Recent combined applications of LiDAR and photogrammetric surveys have made it possible to develop specific methods for locating entrances and producing 3D models and georeferenced plans. The combined use of these models with geomechanical surveys supported by surface seismic surveys makes it possible to understand the state of health of these buried structures and whether, in the event of an earthquake or as a result of natural decay, they could pose a danger to the population. In this work, which builds on recent studies, a method for assessing the state of these cavities is proposed and tested, essentially to evaluate the risks of collapse and sinkholes. The final objective is to census and discover as many cavities as possible, not only for the mitigation of risk but also for the valorisation of these cavities, which represent a true historical and archaeological heritage—testimonies to the history and evolution of ancient Castrum Criptarum.

Keywords: man-made cavities; sinkhole; LiDAR; photogrammetry; geophysics; geomechanics; cavity stability; cavity enhancement

check for updates

Academic Editor: Karoly Nemeth

Received: 14 March 2025
Revised: 7 April 2025
Accepted: 9 April 2025
Published: 11 April 2025

Citation: Gentili, F.; Madonna, S.; Nisio, S. The Importance of the Census of Anthropogenic Cavities in the Mitigation Geological Hazards: The Case of Grotte di Castro (Italy). *Geographies* **2025**, *5*, 19. https://doi.org/10.3390/geographies5020019

Copyright: © 2025 by the authors. Licensee MDPI, Basel, Switzerland. This article is an open access article distributed under the terms and conditions of the Creative Commons Attribution (CC BY) license (https://creativecommons.org/licenses/by/4.0/).

1. Introduction

The Italian territory is characterised, due to its complexity, diversity, and even young geological age, by multiple geological hazards that, due to the widespread presence of infrastructures, cities, housing, and anthropic activities, frequently turn into geological risks. Seismic risk represents perhaps the greatest danger to human activities, and for this reason, it is much studied and regulated by very detailed national and regional regulations [1]. The landslide risk and the flood risk are certainly among the best known and most studied. In Italy, there are no less than 620,000 active landslides, many of which directly affect inhabited centres and infrastructures. In order to try to identify the areas most affected, special planning tools have been drawn up, such as hydrogeological structure plans and flood risk management plans. Without neglecting the volcanic risk, which affects well-defined areas of the Italian territory, there are also risks that, in the collective imagination, are perhaps wrongly, considered minor, such as the sinkhole risk, which consists of the sudden opening of a sinkhole on the surface [2]. This risk is essentially linked to the presence of a cavity, which can be of natural or anthropic origin. In both cases, the creation of the cavity,

whether due to natural or anthropic causes, is closely linked to the characteristics of the geological formation that hosts it [3]. In Italy, many settlements, as well as major cities, are characterised by the presence of historic centres rising on rocky outcrops, modelled by atmospheric agents over hundreds of thousands of years on plateaus raised above the rest of the landscape. These structures, especially in the early Middle Ages, were colonised essentially for defensive reasons, becoming the historic core of most Italian cities and towns. The need to find building materials, destined for the growth of the new settlement, the necessity to have places useful for food preservation and, especially in the Etruscan–Roman and late imperial period, for burial reasons, led to the creation of networks of caves whose construction was interrupted several times in time, only to be resumed according to need in later periods. With the passage of time and due to the absence of a cataloguing and mapping system at the time of realisation, many of these cavities have been lost from memory and are often only rediscovered after, for various reasons related to the state of the vaults, they originate a sinkhole [4,5]. In Figure 1, it is possible to see, in a simplified manner, what the phases are that, with the passage of time, lead from partial collapse of the summit to the formation of a surface sinkhole.

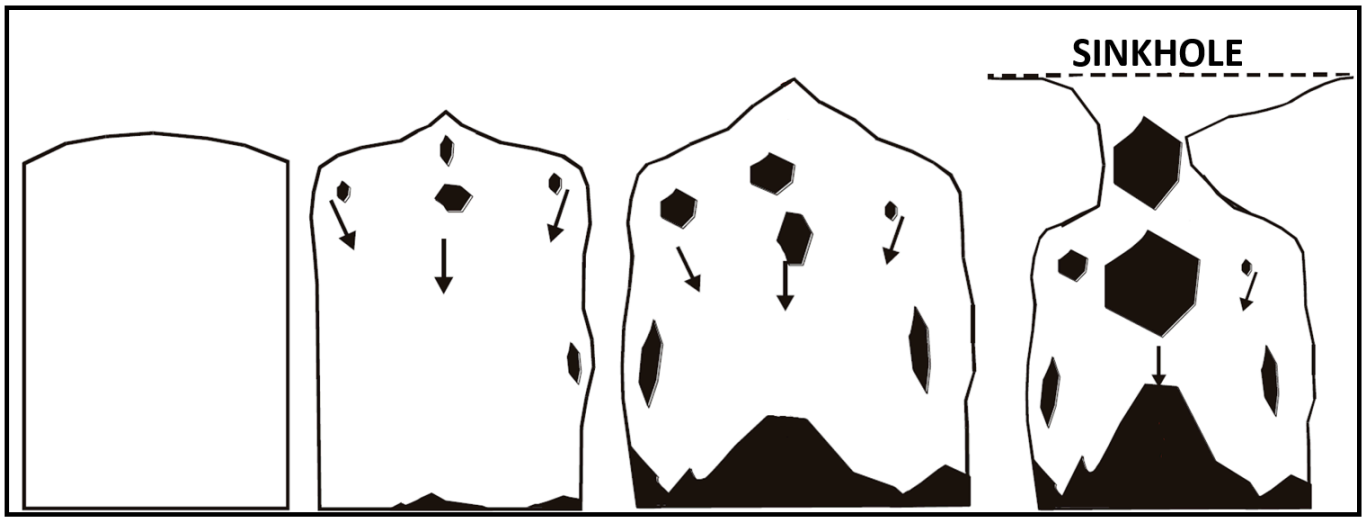


Figure 1. Formation phases of an anthropogenic sinkhole from the collapse of a cavity vault.

In recent years, given the accentuated increase in these phenomena, especially in urban areas, a number of cavity censuses have been initiated in connection with research projects that aim to develop techniques for surveying, monitoring, and assessing the state of these cavities from the perspective of sinkhole hazard. Census and mapping activities of these structures have been conducted in some towns in the Region of Lazio, such as Bolsena [6] and Viterbo [7], essentially relying on traditional research and survey methods, which involve, in addition to irreplaceable archive research, the use of teams in the area and bulky survey instruments used by highly trained personnel. More recently, innovative methods for locating cavity entrances, census and mapping have been developed in Lazio towns, using low-cost photogrammetric and LiDAR surveys. These techniques were developed in the Municipality of Montefiascone [8] and tested in the Municipality of Grotte di Castro [9], where their ease of application and good adaptation to the context were evaluated. The present work follows on the heels of these previous works to provide a combined protomethodology that can be improved over time, leading to the localisation of the cavities, mapping and 3D modelling, insertion in the town context, and stability assessment, while also considering the possible effects that an earthquake could have on these structures. The aim is to understand, starting from the census, which are the weakest parts of these cavities that could potentially generate sinkholes in the urban fabric. The

results of the census of the cavities in a portion of the built-up area of Grotte di Castro are reported below, and possible methods are suggested for evaluating the stability of these structures, which are closely linked to the potential and success of the mapping. The ultimate goal, which can only be achieved with a complete census, is to know and assess the stability and the possible valorisation of these cavities with a view to sustainability and renewal of the urban fabric.

2. Study Area

The activities of survey and inventory were carried out in the historic centre of the Municipality of Grotte di Castro, which has already been the subject of recent studies and the application of modern geophysical and photogrammetric techniques for the research and study of anthropic cavities [9,10], with the present work being a continuation of these efforts. Secondly, the historic centre is almost entirely marked as a zone of attention due to the presence of cavities catalogued in the Hydrogeological Asset Plan of the Central Apennine Basin District Authority [11] and the identified risk of landslides. Therefore, it was deemed useful to deepen this type of study in an area with identified critical issues, with the aim of providing a contribution, albeit limited and experimental, to the assessment of sinkhole risk in these areas.

2.1. Geological and Geomorphological Settings

The study area is located north of the Latium Region in central Italy (Figure 2A), where geological formations belonging to the Latera Volcanic Complex (Figure 2B,C), part of the Quaternary Vulsini Volcanic District (VVD), are present. located in the Roman Alkaline–Potassium Magmatic Province, a band of young volcanoes along the west coast of Italy [12]. This district is characterised by multicentre volcanic complexes, calderas (e.g., Latera and Montefiascone), and extensive eruptive activity that has produced more than 40 km^3 of volcanic materials, including ignimbrites, pyroclastic deposits, lavas, and cinder cones [13–15]. The composition of the rocks varies from trachybasalt potash to phonolite. This district developed along a graben and horst system, with pre-volcanic rocks belonging to the Ligurian, Tuscan, and Umbrian sequences. Five main volcanic complexes have been identified: Paleo–Vulsini (1.3–0.49 million years ago), Bolsena–Orvieto (0.49–0.3 Ma), Montefiascone (0.3–0.2 Ma), Latera (0.28–0.14 Ma) and the Southern Vulsini (0.4–0.13 Ma) [16]. The beginning of volcanism shifted around 1.7 million years ago. Grotte di Castro is located on a plateau formed by pyroclastic deposits shaped by fluvial processes during the Last Glacial Maximum. The upper tuffaceous complex of Latera includes the Grotte di Castro, Onano/Poggio Pinzo, and Pitigliano formations, while the lower tuffaceous complex includes the Sorano, Sovana, Farnese, and Canino formations [9]. These formations, classifiable as soft rocks, are easily eroded and present fracture planes due essentially to the cooling that occurred after setting and to the action of atmospheric agents that widen these already present fractures. In later times, the action of vegetation further contributes to widening these fractures, causing landslides by collapse and overturning of the stone material. Furthermore, these formations in the past and today have been used as construction material because they are easy to work, favouring underground excavations for this purpose as well. The underground cavities studied developed mainly in the Grotte di Castro and Sorano formations, characterised by consolidated ash flow deposits, pumice and lithic.

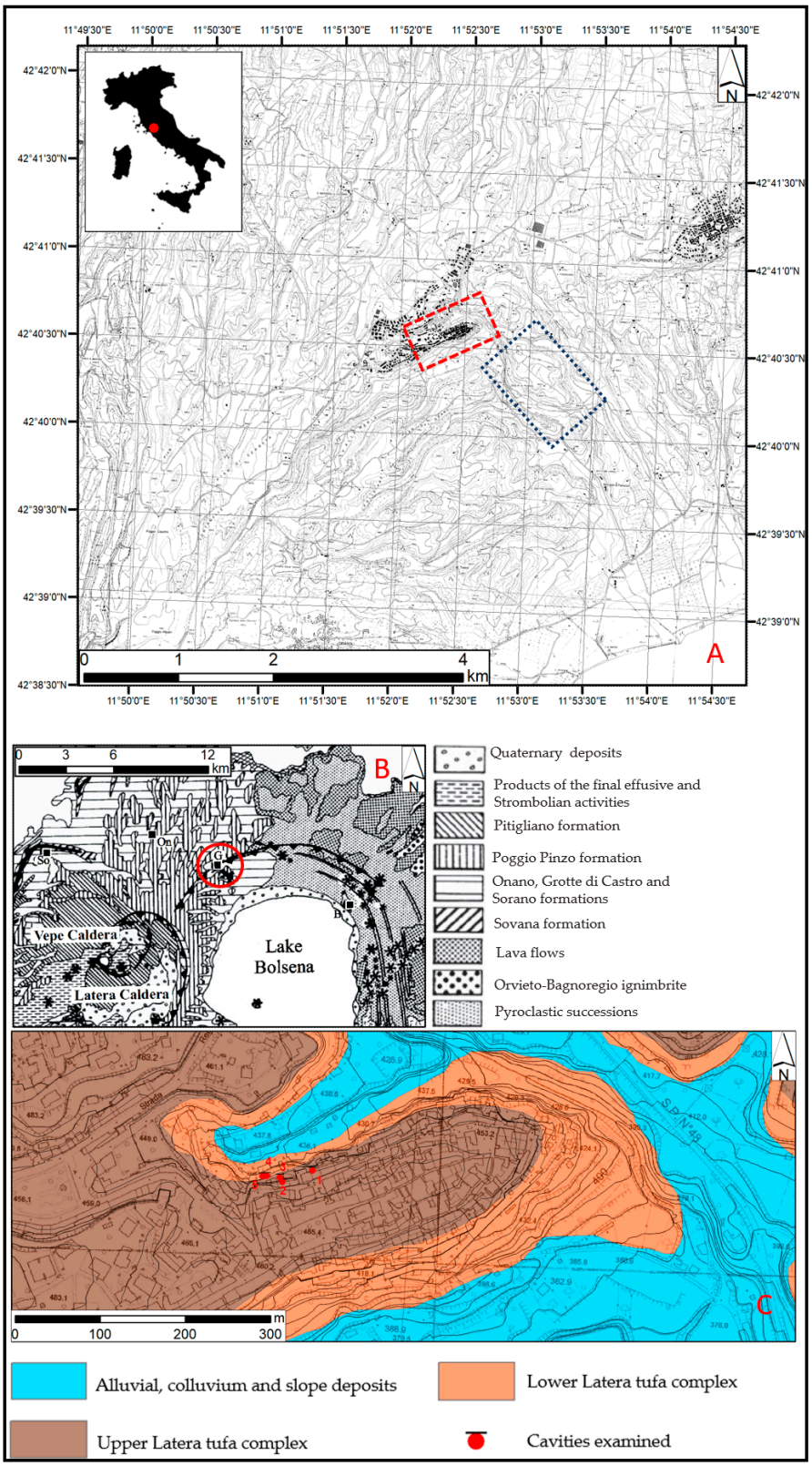


Figure 2. In the red rectangle, the current historical centre of Grotte di Casto and study area is highlighted, and in the blue rectangle, the site of the ancient Civita of Grotte di Castro (geographical coordinates wgs 84) (**A**). Portion of interest of VVD, in the red circle the area of Grotte di Castro (from Acocella et al. 2012) (**B**). Geological map of the area by Gentili and Madonna 2024 (detail in the red rectangle of (**A**,**C**)).

2.2. Historical Notes on the Evolution of Grotte di Castro and Its Cavities

The first Etruscan settlements date back to around the 7th century B.C. and are located in the area that is now known as Civita di Grotte di Castro (Tiro in antiquity—Figure 2A). Situated in a frontier area and developed thanks to its connections with the territories of Vulci, Tarquinia, and Vulsini [17]. Civita experienced a phase of economic and demographic growth in the Etruscan period, as testified by the numerous finds discovered in the area [18,19]. The most recent archaeological mapping [20,21] details the Etruscan necropolises' locations outside Civita. Around 300 B.C., with the first Roman incursions, there was an initial decline of the settlement, which, however, managed to prosper for the next 870 years [22]. With the arrival of the Lombard invasions in 572 A.D., Civita was completely abandoned. It was a violent phase with the killing of a large part of the population in the Valley of the Screams [23]. During this period, the surviving population settled in the present town centre. The demand for building material probably coincides with the first excavations of the caves on both the northern and southern slopes, so much so that in the document of donation to the Holy See by Matilda of Canossa, the settlement is defined as Castrum Criptarum, which can be literally translated as citadel of the crypts [24]. Excavations of caves proceeded throughout the Middle Ages and much of the Renaissance, where the demand for building material was replaced by the need to store food and wine for long periods. For this reason, excavations along the northern side were favoured, which for microclimatic and exposure reasons favoured better food preservation. No sources were found at the end of the excavations. Still, it is possible to estimate the total duration of the operations to be between 700 and 1000 years, during which operations were repeatedly resumed and interrupted.

2.3. Climatic Notes

According to the Köppen–Geiger climatic classification [25], Grotte di Castro has a warm-temperate climate, with a dry season in the hot quarter and an average temperature of the hottest month above 22 °C (Csa). The average annual temperature is around 13.8 °C, while the average annual rainfall is around 1000 mm. To better understand the climatic conditions of the study area, the SIARL—Integrated Agrometeorological Service of the Lazio Region (https://www.siarl-lazio.it/index.asp, accessed on 2 March 2025)—was consulted. Of the stations present on the territory of the municipality of Grotte di Castro, the one in the locality of 'Purgatorio' was selected, located at the WGS84 coordinates 42°41′03.98″ N 11°52′54.61″ E at an altitude of 470 m asl. This station was chosen because it is spatially closer and at a similar altitude to the study area. From the available time series analysis dating back to May 2008, a climatogram for this area was constructed. (Figure 3).

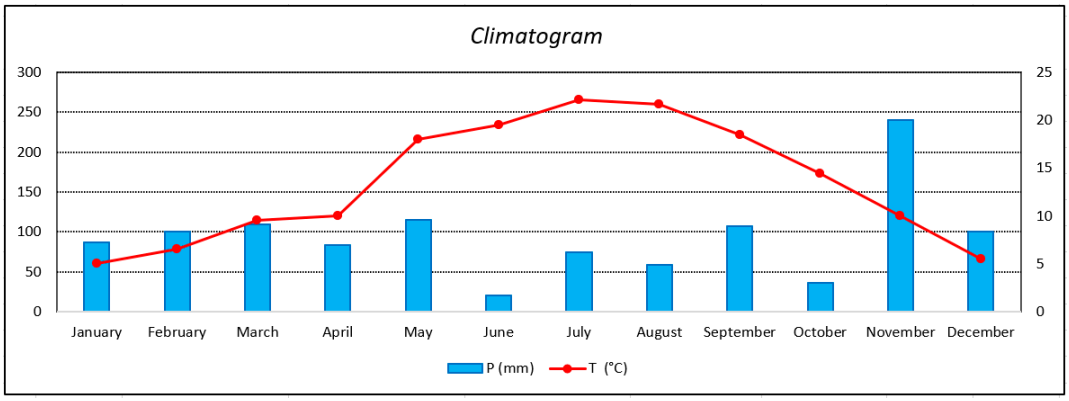


Figure 3. Climogram of Grotte di Castro reconstructed based on data from the weather station in the 'Purgatorio' area.

Based on the climatogram analysis, there is a fairly even distribution of precipitation in the first part of the year. With the exception of the months of June and September, which, respectively, mark the lows and highs of the hot period, substantial equidistribution is also found in the summer phase, clearly characterised by smaller volumes than in the first five months of the year. The final part of the year is very unbalanced in terms of rainfall, with October experiencing little rain, November being rich in precipitation, and December being more in line with the statistics of the first part of the year. Temperatures have a more regular trend, although moderate increases are recorded, especially in the months following the summer. On average, there are about 95 rainy days per year.

3. Materials and Methods

The applied method, of a multidisciplinary nature, was seen as the first step in the choice of intervention area. Grotte di Castro was selected for the reasons listed in the Introduction, concerning the presence of previous studies that could be used as a starting point and the objectively present risk and danger conditions. Of the two sides of the cliff, the northern side was selected because, based on historical archaeological documentation, it is probably affected by a greater number of cavities. Access was gained to five cavities. These cavities are arranged on several levels; in detail, 1 and 2 are on the highest level, 3 on the middle level, and 4 and 5 on the lowest level (Figure 2B). The second step was to select the field data acquisition area based on possible access to the cavities. The field data acquisition part saw the execution of photogrammetric surveys of Grotte di Castro, LiDAR (Light Detection and Ranging) surveys of the cavities, surface seismic surveys to study the properties of the rock mass, and geomechanical and joints surveys inside the cavities. The processing phase saw the combined use of data obtained from 3D models, seismic and geomechanical surveys, combined with different methods for assessing the stability of the cavities, essentially empirical in nature, simplified in number, and through the use of special software. Experimental numerical modelling from a seismic perspective was also attempted, using the provisions of the Italian national regulations. The aim was to produce an initial map of susceptibility to collapse of the vaults. The individual methods used are presented below.

3.1. Photogrammetric and LiDAR Surveys

Photogrammetry, which is used for land modelling and the production of detailed maps, is now a reliable and rigorous tool [26], capable of returning surveys characterised by centimetric accuracy and adaptable to different problems [27,28]. Photogrammetric surveys were performed using the DJI Mavic Pro UAV model (produced by Dà-Jiāng Innovations Shenzhen—China) armed with a 12-megapixel on-board camera. Photographic acquisitions were carried out in nadiral (camera oriented at $-90°$) from a speed of 3 m/s and at an altitude of 30–35 m above ground level, with an estimated photographic overlap of around 75%. The frontal acquisition images (camera oriented between $-30°$ and 0) were taken under the same flight conditions. A total of 965 images were acquired. To avoid problems related to city traffic, the flights were carried out after 9.30 a.m., selecting days with good cloud cover and no wind. The survey was supported by the placement of appropriate markers (Figure 4), the centre of which was surveyed with a Leica GNSS station consisting of a CS10 controller, GS08 plus rover and a two-metre rod. The photogrammetric process was carried out using the Agisoft Metashape software [29], version 1.6.3. LiDAR surveys were carried out using the iPhone 15 Pro Max, which mounts a Sony IMX591 ToF-type SPAD sensor (produced by Sony Group Corporation Tokio—Japan). Access was gained to 5 cavities that were surveyed using the iPhone only (Figure 5). The effectiveness of this tool has been tested in numerous works [9,30,31] and also for surveying city utility networks [32].

The LiDAR surveys were carried out using two markers (Figure 4), one in common with the UAV survey and one within the cavities to facilitate alignments of multiple sections. A portable light source was used during the LiDAR survey to aid acquisitions. The acquisition and processing were carried out using the Scaniverse application. The models and point clouds of the individual cavities were aligned to the point cloud and model obtained from the UAV survey, which served as a reference. The alignment was performed using the Cloud Compare software (version 2.1), through the Alings Two Clouds tool [33].

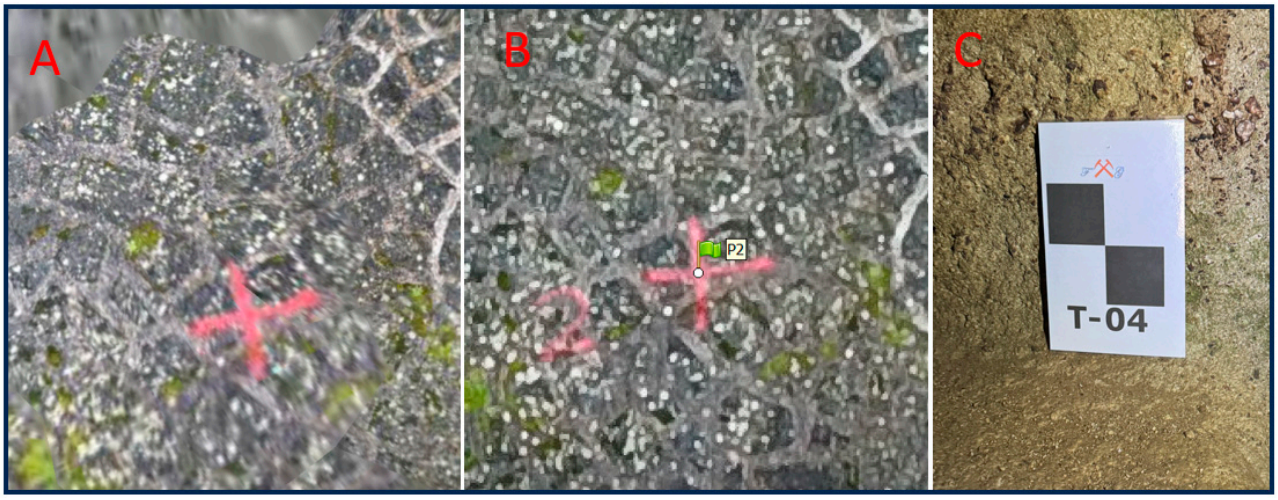


Figure 4. Marker used to align LiDAR and photogrammetric models (taken from LiDAR model) (**A**); the same marker is used to geo-reference the photogrammetric survey (taken from photographic image) (**B**); and marker used in cavities to aid alignments (**C**).

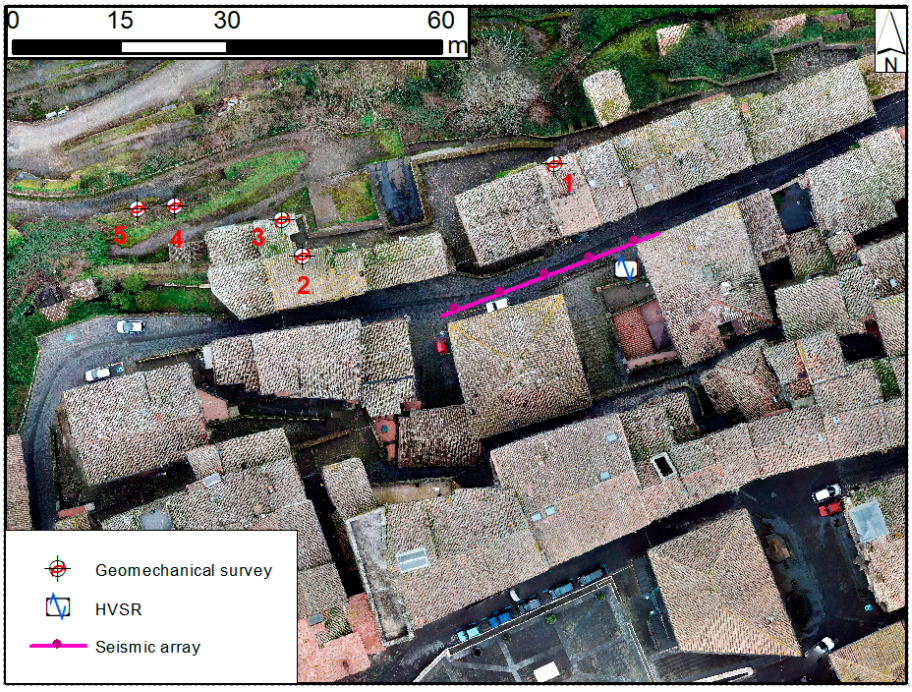


Figure 5. Positioning of seismic and geomechanical surveys on orthophotos from photogrammetric relief. Geomechanical survey symbols are positioned at the cavity entrances.

3.2. Seismic Surveys

The seismic investigations involved the use of multiple techniques to obtain reliable measurements of the P-wave velocity (Vp) of the S-waves (Vs), which were used to determine the Poisson coefficient. Microtremor measurements were also carried out to estimate

the site frequency (f_0) to obtain a more complete picture of the seismic properties of the rock mass hosting the cavities. For all acquisitions and processing, the recommendations and guidelines provided by the C.N.R. (National Research Council) [34] and the SESAME project were followed, especially for microtremors [35]. The methodologies used were as follows:

- Refraction Seismic. Generalised Reciprocal Method (GRM) [36] was used to measure Vp. The instrument used was the seismograph model DoReMi from Sara Elettronic Instruments, equipped with 16 vertical 4.5 Hz geophones, with an intergeophonic distance of 2 m. Seven bursts were made, using a 5 kg sledgehammer on a steel plate as energiser. Burst distances were set, relative to the first geophone of the array at −5 m, −1 m, 5 m, 15 m, 25 m, 31 m, and 36 m. The open-source software smartRefract 2017 was used for interpretation.
- MASW. The Multi-channel Analysis of Surface Waves [37] method was used to measure Vs using the same instrument, array, and energisation mode. The burst distance was set at 3 m, 5 m, and 7 m from the first geophone, and the different acquisitions were compared to each other after processing using the open-source software Geopsy and Dinver [38], versions 3.4.0 [35].
- HVSR. The Horizontal to Vertical Spectral Ratio method [38] was used to measure the site frequency f_0 using the 3-channel Geobox seismograph from Sara Elettronic Instruments with 4.5 Hz geophones. The instrument is north-facing and levelled, and the acquisition of microtremors lasted for 25 min. The test processing was carried out using the open-source software Geopsy (version 3.4.). All windows with anthropogenic noise and disturbed signal were removed during the processing.

The S-wave and P-wave velocities were used to estimate the Poisson's coefficient (ν), according to the following equation [39]:

$$\boldsymbol{\nu} = \frac{\boldsymbol{Vp^2 - 2Vs^2}}{\boldsymbol{2(Vp^2 - Vs^2)}}. \quad (1)$$

Figure 5 shows the location of the investigations.

3.3. Geomechanical Surveys and Rock Mass Classification

A geomechanical survey was performed in each cavity to determine the rock mass parameters, its classification according to Barton's method [40] and the measurement of joints (Figure 5). Using the Gestone rock sclerometer (produced by Novatest S.r.l Ancona—Italy), the rock's uniaxial compressive strength (σc) was estimated. Where the rock mass was very poor, it was impossible to carry out measurements with the rebound index sclerometer because the rebound index gave full-scale values beyond the instrument's calibration. To overcome this problem, ISMR standards were used [41,42]. The joints were detected by measuring the dip direction and the inclination, using the geologist's compass. The Barton classification was made by determining the parameter Q according to the following equation:

$$\mathbf{Q} = \left(\frac{\mathbf{RQD}}{\mathbf{Jn}}\right) \times \left(\frac{\mathbf{Jr}}{\mathbf{Ja}}\right) \times \left(\frac{\mathbf{Jw}}{\mathbf{SRF}}\right), \quad (2)$$

where

- **RQD** (rock quality designation) considers the rock mass's subdivision;
- **Jn** (joint set number) depends on the number of joint families present in the rock mass;
- **Jr** (joint roughness number) depends on the roughness of the most unfavourable family;

- **Ja** (joint alteration number); depends on the degree of fracture alteration, thickness and nature of the fill, and which is also determined by the most unfavourable family;
- **Jw** (joint water number) wich depends on hydrogeological conditions;
- **SRF** (stress reduction factor) is a function of the stress state in massive rocks or tectonic disturbance

To estimate the rock mass parameters according to Hoek and Brown's criterion [43,44], the Geological Strength Index (GSI) [45] was also estimated by applying the method suggested by the authors.

3.4. Stability Assessment

Various methods were used to assess the stability of the surveyed cavities, involving different approaches and deeper knowledge about the rock mass and the geometry of the cavities. Empirical methods, simplified numerical modelling methods, and computer-aided methods were used. The following were selected for the empirical methods.

- Critical Scaled Crow Span Method. The method proposed by Carter [46,47] proposes to assess the stability of a cavity vault by calculating the scaled crow span Cs, which if it is greater than critical span Sc then unstable conditions exist. The parameters are calculated according to the following equations:

$$\mathbf{Cs} = \sqrt{(\boldsymbol{\gamma}/\mathbf{T}\left(\mathbf{1} + \frac{\mathbf{S}}{\mathbf{L}}\right)(\mathbf{1} - \mathbf{0.4cos\theta}))}, \quad (3)$$

where

- **S** = clear span of the vault in metres;
- **L** = length of the vault in metres;
- **T** = thickness of the vault in metres;
- γ = specific gravity of the rock mass (17–18 kN/m^3);
- θ = deep direction of the stratification.

$$\mathbf{Sc} = \mathbf{3.3Q^{0.43}}\left(\mathbf{senh^{0.0016}(Q)}\right), \quad (4)$$

where **Q** is determined by Barton classification.

- Harp and Noble method. It examines the propensity for slope collapse in a seismic event with M > 5 [48]. The methodology is based on Barton Q parameter, modified by the following equation:

$$Q'' = \left(\frac{(\mathbf{115} - \mathbf{3})Jv}{Jn}\right)\left(\frac{Jr}{Ja}\right)\left(\frac{\mathbf{1}}{AF}\right), \quad (5)$$

where

- **Jv**: are number of joints per m^3;
- **AF**: considers the discontinuity's opening.

The value of Q'' indicates the susceptibility to collapse in the event of an earthquake on a scale from low to high.

The voussoir beam analogue was applied for simplified calculation methods, assuming a continuous elastic beam [49,50]. Although this model is explicitly designed for stratified masses, it can also be used for the type of mass under examination, since it is present in the horizontal stratifications typical of many ignimbritic cliffs in the other Lazio region. However, this is a borderline case, which is useful, when compared with other systems, to begin to assess the real applicability of this method to this type of rock and excavation. According to this method, the vault can be modelled as a beam, the thickness of which is

given by the thickness of the stratification. The following equation gives the tensile stress exerted on the beam:

$$\boldsymbol{\sigma s} = \frac{\gamma z L^2}{2h^2}, \quad (6)$$

where

- $\boldsymbol{\gamma z}$ is the lithostatic load;
- L is the length of the vault;
- h is the rock layer thicknesses.

A safety factor can be determined by comparing the value of the rock tensile strength σt with the value of σs. Since reliable values of σt from laboratory tests are not available, this parameter was evaluated by considering 20% of σc as a precautionary measure. This modelling was applied to the cavity halls. The software Examine^{2D} (version 8.0), a 2-dimensional plane strain boundary element programme for the elastic stress analysis of underground excavations, was used for the computer simulations. The input data are topography, cavity geometry, and rock mass parameters according to Hoek and Brown or Mohr–Coulomb criteria, rock volume weight and Poisson's coefficient. Information about the joints, which can be parameterised according to Barton's criterion [51], can also be included if the position and persistence is known with good approximation. Given the availability of seismic surveys, an attempt was also made to model the stability of the cavities from a seismic point of view. To this end, topographic and stratigraphic seismic amplification coefficients were calculated, as required by Italian regulations [1]. These values were useful in estimating the surface seismic acceleration, calculated from the seismic acceleration at bedrock (Vs > 800 m/s), reported from the INGV (National Institute of Geophysics and Volcanology) interactive seismic hazard maps [52,53]. As input data, the coordinates of Grotte di Castro and an earthquake with a return time of 475 years, indicated by the Lazio Region Civil Protection guidelines as the maximum expected event [54], were selected. Finally, the use class was determined as a final parameter, which considers the structure's crowding and use, attributing crowding from low to normal. The calculated surface acceleration was then used to evaluate, in a simplified way, the increase in loads induced by an earthquake thus hypothesised, again applying the methods foreseen by the above regulations [1]. These new data were entered into Examine^{2D} to evaluate a possible earthquake scenario hypothetically. Since this software works in two dimensions, several sections were taken (one every 4 m) to assess the variation in safety coefficients along the cavity path and in the immediate surroundings. In addition to simulating the stability conditions for each individual cavity, safety factors were also estimated by considering all surveyed cavities along a section deemed representative. To do this, previously surveyed and surveyed cavities were also considered and reported in Gentili and Madonna 2024 [9]. The orientation of the joints in the rock mass was considered by studying the alignment of the cavities in Cloud Compare. Using the software's Compas plugin (Cloud Compare version 2.1), the joints were highlighted and directions in the cluster were assumed. Everything was then brought back into the CAD environment where the input .dxf file for Examine^{2D} was prepared.

4. Results

4.1. LiDAR and Photogrammetric Surveys

From the photogrammetric survey, the point cloud (Figure 6A), the textured 3D model, the orthophotos, and the digital elevation model were obtained, with elevations expressed in metres above sea level according to the Italgeo 2005 Geoid model, reported in the GK2 IGM (Istituto Geografico Militare) grid used to process the GNSS station data. The errors associated with the photogrammetric survey were 3.8 cm on GCP and 4.6 cm on CP.



Figure 6. Point cloud from photogrammetric survey in Cloud Compare (**A**). Cavity n5 surveyed with iPhone LiDAR in Cloud Compare (**B**).

The LiDAR surveys of the cavities were aligned with the drone survey (Figure 7). Table 1 shows the errors calculated by the Cloud Compare software (Cloud Compare version 2.1), in terms of RSM and scaling factors for each surveyed cavity. All the cavities examined were excavated with hand tools, the signs of which are evident on the walls. They also present the same organisational structure, which can be subdivided into an alternation of main rooms connected by long, narrow connecting structures.

Table 1. Errors associated with the alignment of the reliefs and scale factors.

Cavity	Error (RMS cm)	Scale Factor
1	1.6	0.996
2	3.1	1.004
3	2.1	0.999
4	2.3	0.998
5	2.1	1.001

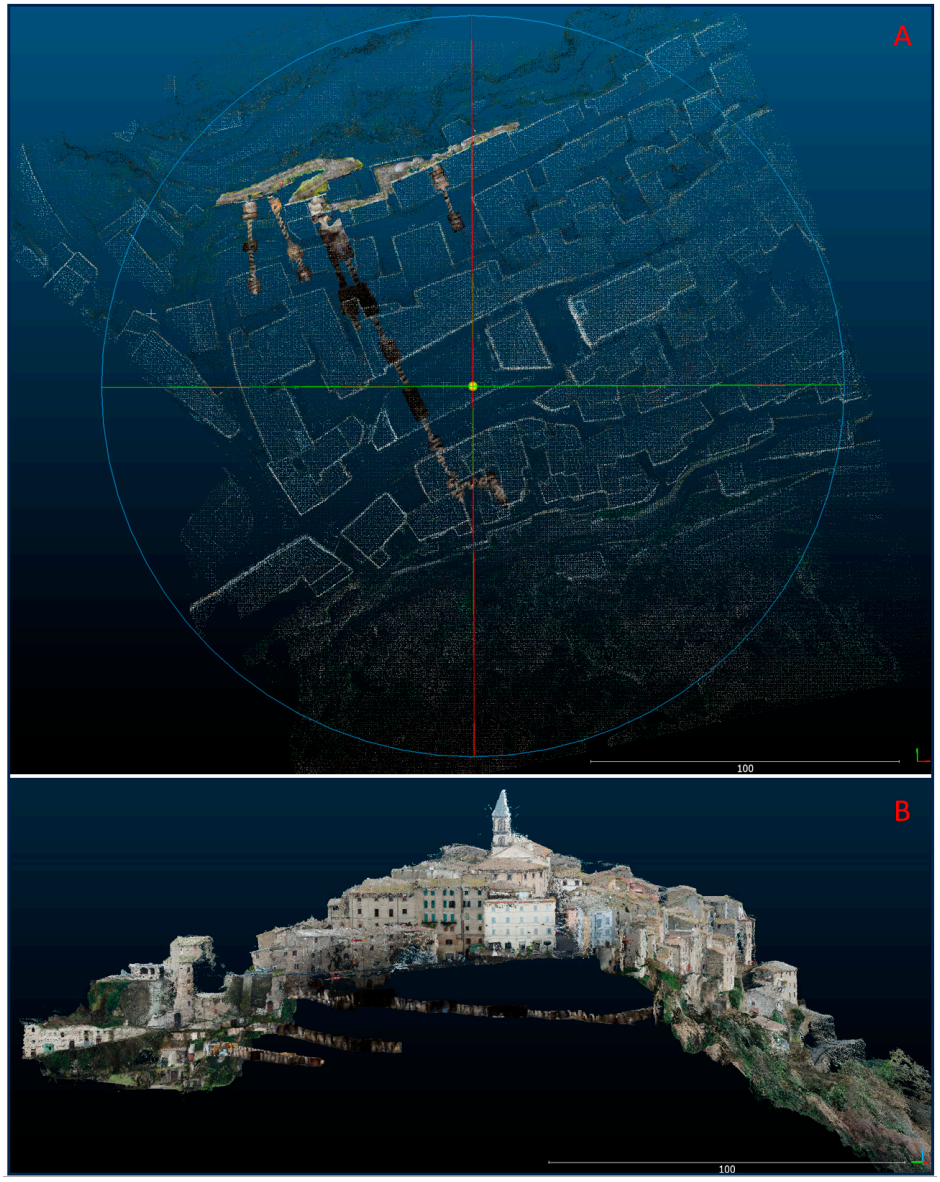


Figure 7. Alignment of models and clouds in nadir view (**A**) and in section (**B**).

4.2. Seismic Surveys

From the seismic analyses, the P-wave and S-wave velocities were obtained. Refraction seismics provided Vp information for two identified seismostrata (Figure 8A). In particular, a seismostratum with a Vp of 809 m/s, with thicknesses between 2 and 5 m, and a seismostratum with a Vp of 1126 m/s, with thicknesses probably greater than 6 m, were found from the section. The MASW investigation produced a seismostratigraphy of three seismic layers, one with a thickness of 3 m with Vs of 372 m/s, one with a thickness of 19 m with Vs of 512 m and a third with Vs of 725 m/s and thickness greater than 8 m (Figure 8B). According to the Italian standard, it is possible to estimate a Vs30, which would be the weighted Vs velocity in the first 30 m, of 533 m/s corresponding to a B category (360 m/s < VS < 800 m/s). The site frequency detected by the HVSR test is 1.35 Hz (Figure 8C), which places the possible location of a seismic substrate (Vs > 800 m/s) at an estimated depth of between 70 and 90 m from ground level [55]. The SESAME criteria confirm that the H/V curve and the peak are reliable (Figure 8D). A Poisson's coefficient of 0.36 can be calculated for both seismic layers, which makes it possible to know both Vs and Vp.

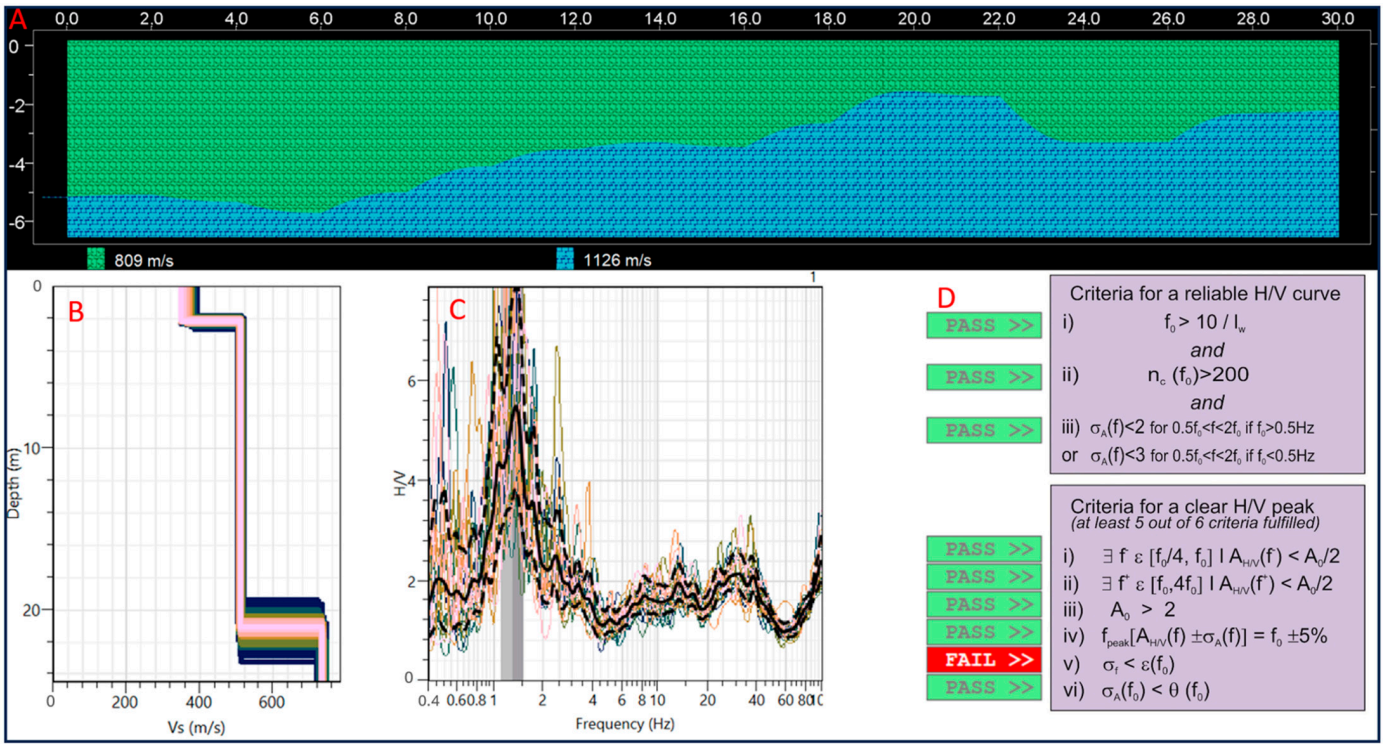


Figure 8. Refraction seismic section. (**A**) In green, the superficial layer with lower Vp is highlighted, and in blue, the deeper one with higher Vp, the test reaches almost 7 m and for the 30 m array length. Seismostratigraphy from MASW (**B**) representing Vs (in m/s) with depth (the test explores almost 30 m from ground level). HVSR curve, with peak frequency indicated in grey (**C**). SESAME criteria of curve and peak reliability (**D**). According to these criteria, both curve and peak are considered reliable.

4.3. Geomechanical Surveys and Rock Mass Classification

The geomechanical study of the cavities made it possible to define, albeit locally, the properties of the rock mass. In particular, three different quality levels were found, characterised by different Q and σc values. The first quality of the rock mass is the most superficial, hosting the cavities of the first level. The second quality is ideally located below the first and hosts the cavities of the second and third levels. Finally, the third quality is located within the cliff of Grotte di Castro and was studied within cavity no. 2 (from the middle onwards), which, due to its extension, almost completely crosses the cliff from north to south. Table 2 shows the cluster classifications with parameters. The volume weights were based on previous neighbouring investigations that estimate this parameter to be between 17 and 18 kN/m^3.

Table 2. Rock mass classification and parameterisation.

Quality Level	Q	Class	GSI	σc (MPa)	σt (MPa)
1	2.43	Poor	53	8	1.6
2	7.51	Fair	58	10	2
3	0.45	Very poor	50	5	1

The fractures surveyed essentially belong to two families that are found in the studied cluster in equal measure and are, respectively, characterised by dip direction and dip 175°/71° and 352°/68°. These are average values that define the main orientations of these joints. In addition to these, there are high recurring fractures that cannot be categorised into main families, such as 25°/68° or 90°/71°. All of the fractures are persistent and

sometimes have openings of over 5 cm. Figure 9 shows the stereogram with some of the main fractures surveyed.

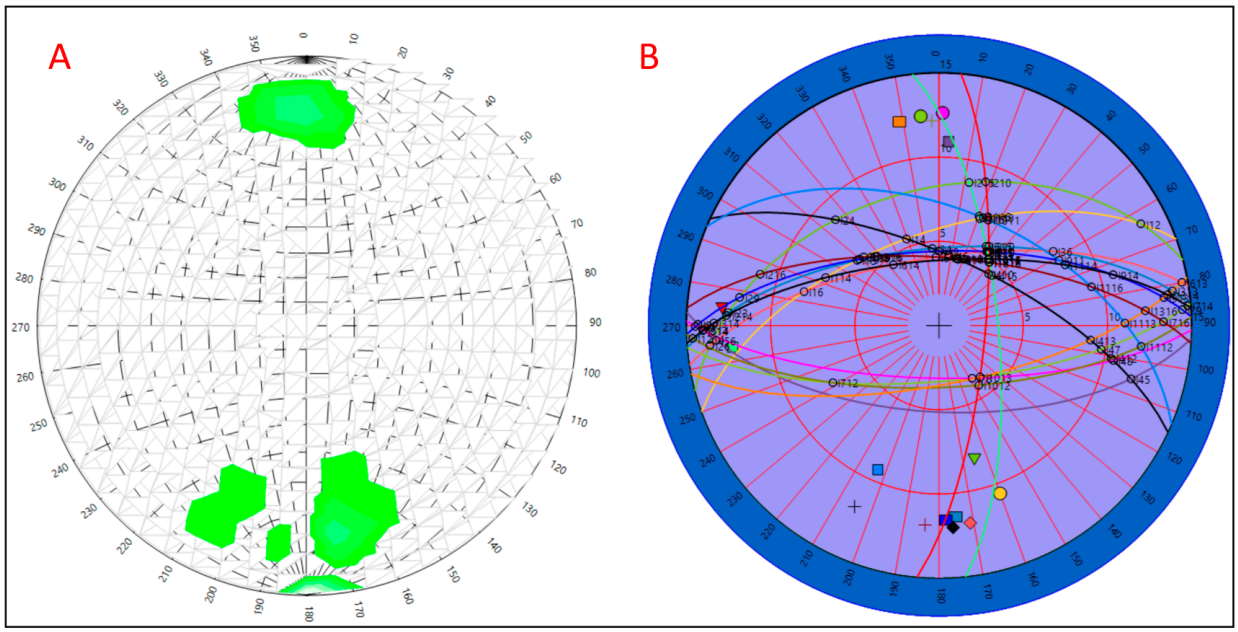


Figure 9. Stereograms with density of joints poles (in light green the areas with the highest concentration of poles (**A**) and with representation in cyclography (**B**). The stereograms indicate the spatial arrangement of fractures within the rock mass and give information about possible landslides that may occur along the fractures.

4.4. Stability Assessment

Below are the results of the stability of the halls and connection structures of the individual cavities according to Carter's method (Table 3). The geometric parameters were taken from the 3D model obtained by combining the cavity and surface models.

Table 3. The results of Carter's method.

Cavity	Part	Cs	Sc	Stability (Cs < Sc)
1	Connection 1	0.67	5.09	Yes
	Room 1	1.87	5.09	Yes
2	Room 1	5.00	5.09	Yes (limit)
	Connection 1	1.06	5.09	Yes
	Room 2	2.88	5.09	Yes
	Connection 2	0.90	5.09	Yes
	Room 3	2.27	5.09	Yes
	Connection 3	0.66	2.35	Yes
	Room 4	1.76	2.35	Yes
	Connection 4	0.70	2.35	Yes
	Room 5	1.57	2.35	Yes
	Connection 5	0.84	2.35	Yes
	Room 6	2.88	2.35	No
	Room 7	2.37	2.35	No
	Room 8	2.78	2.35	No
3	Connection 1	1.03	7.93	Yes
	Room 2	2.07	7.93	Yes

Table 3. *Cont.*

Cavity	Part	Cs	Sc	Stability (Cs < Sc)
4	Room 1	3.73	7.93	Yes
	Connection 1	1.36	7.93	Yes
	Room 2	2.02	7.93	Yes
	Connection 2	0.87	7.93	Yes
	Room 3	1.62	7.93	Yes
5	Room 1	3.73	7.93	Yes
	Connection 1	1.36	7.93	Yes
	Room 2	2.02	7.93	Yes
	Connection 2	0.87	7.93	Yes
	Room 3	1.62	7.93	Yes

Table 4 shows the results of the Harp and Noble method, evaluating the possibility of collapse in reference to a magnitude 5 earthquake. This assessment, being linked to Barton's Q, is made not by cavity but by rock mass quality.

Table 4. The results of the Harp and Noble method.

Class (Q)	Q″	Susceptibility
Poor	9.7	Medium
Fair	5.8	Medium
Very poor	2.2	Medium

Table 5 shows the results of the simplified numerical method. Again, unified 3D model were used to estimate thicknesses (and thus lithostatic loading) and cavity geometries.

Table 5. The results of the simplified numerical method.

Cavity	Part	σs (MPa)	σt (MPa)	SF (σt/σs)
1	Room 1	0.57	1.60	2.82
2	Room 1	1.11	1.60	1.45
	Room 2	1.44	1.60	1.11
	Room 3	1.34	1.60	1.19
	Room 4	1.85	1.00	0.54
	Room 5	0.81	1.00	1.24
	Room 6	1.35	1.00	0.74
	Room 7	1.20	1.00	0.84
	Room 8	1.11	1.00	0.90
3	Room 1	1.07	2.00	1.86
4	Room 1	0.15	2.00	13.20
	Room 2	0.30	2.00	6.70
	Room 3	0.27	2.00	7.28
5	Room 1	0.31	2.00	6.45
	Room 2	0.94	2.00	2.12
	Room 3	0.63	2.00	3.17

The simulations with Examine^{2D} resulted in 61 sections in which the factors of safety for the areas around the excavation were examined. A factor of safety was assigned to the cavity ceilings by considering the space between two sections as homogeneous and derived from the average values from the two adjacent sections, where the simulations returned a value of less than 1. This was carried out both in static and in the seismic simulation mode proposed here. In almost all of the cavities, there are few areas of instability; they are spaced out, punctiform, and localised, especially in the areas richer in joints. Under seismic

conditions, these areas increase in surface area and involve larger vault portions. Cavity n2 deserves separate treatment, showing contiguous instability in the innermost halls and corridors. From a seismic point of view, there is a susceptibility to collapse that affects almost 1/4 of the total surface of the vault, also involving larger volumes (Figure 10B,D). Table 6 shows the values expressed in percentages concerning the entire surface area of the cavity vault. These measurements were performed in a GIS environment using QGIS software (version 3.16) [56]. The expected seismic acceleration at the bedrock, referred to an earthquake with a return period of 475 years, for the area under investigation is 1.38 m/s^2 (0.14 g), which becomes 1.99 m/s^2 (0.2 g), considering a topographic category T2 and a soil category B [1].

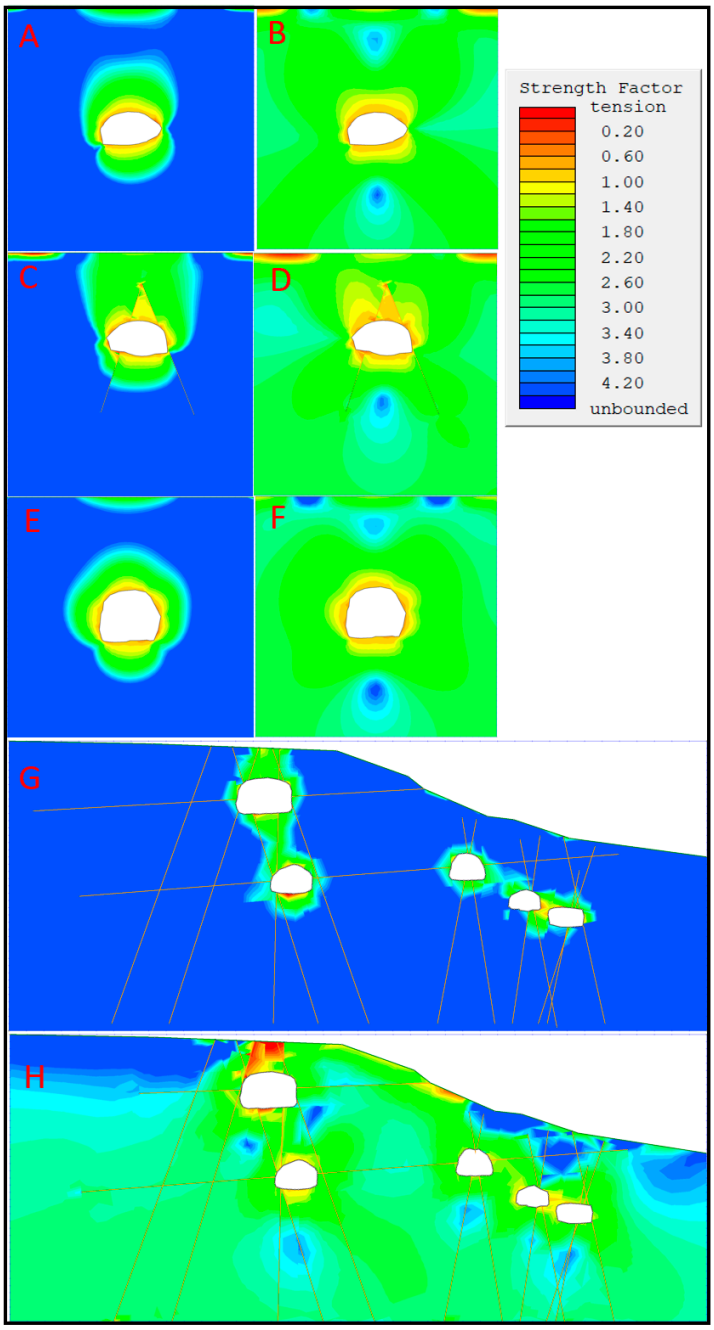


Figure 10. Section of room 6 of cavity 2 in static (**A**) and seismic (**B**) optics. Section of room 7 of cavity 2 in static (**C**) and seismic (**D**) optics. Section of room 2 of cavity 4 in static (**E**) and seismic (**F**) optics Overall section in static (**G**) and seismic (**H**) optics. Strength factors with orange to red colouring indicate unstable areas prone to collapse.

Table 6. Percentage of cavity vaults with safety factor less than 1.

Cavity	SF < 1 (Static)	SF < 1 (Seismic)
1	2.6%	4.4%
2	12.3%	26.3%
3	2.5%	3.9%
4	1.6%	2.8%
5	1.8%	3.3%

Figure 10 shows the results of some simulations with Examine^{2D} for some sections of the cavities, both in static optics and in the attempt made here for seismic optics.

5. Discussion

The historical centre of Grotte di Castro is affected by numerous man-made cavities, excavated during the Middle Ages and Renaissance in the tuffaceous cliff that hosts the town. This excavation activity can be traced back to two main motivations: the need to find building material for urban development and the preservation of food over time. This excavation activity is described in various historical and archaeological documents, which, as reported in recent works [57], represent a solid starting point for the research of these caves. It is precisely based on these sources that a study area was selected, based also on the actual availability of access, to refine methods of census and modelling of the cavities to learn about their state of health, the possible risks associated with their presence, and also to be able to assess in the near future their possible use for public enjoyment. Using now-standardised methods of photogrammetric survey using UAVs and LiDAR with low-cost, but precise and accurate instruments within short distances (maximum 5 m), it was possible to reconstruct a 3D model of the cavities involved in the study and contextualise them in the cliff, capturing the interactions with the surface. Thanks to the centimetric error associated with these models, it was possible to obtain reliable and repeatable measurements in any section of the cavities, obtaining precise information about the thicknesses of the vaults, the geometries and the course of these ancient excavations in the tuffaceous plateau. Combining these products with geomechanical surveys and seismic investigations is an effective way of knowing the rock mass parameters, making it possible to assess the degree of stability of these excavations. Applying geotechnical methods made it possible to classify the rock mass into three qualitatively different types.

According to Barton's method, a first surface layer was identified as poor, resting on other qualitatively better layers. This is also confirmed in publications on local stratigraphy, which attribute a lower degree of compactness to the surface formations. The third quality of the rock mass was found within cavity n2 and is the most geotechnically poor. The least qualitative formations are located near the south cliff of Grotte di Castro, a place characterised by a smaller number of cavities that present cracks and collapses in greater numbers than those on the north side. Numerous buttresses and retaining walls along the roads on the south side testify to this geological fragility. The seismic surveys, carried out to determine certain parameters of the rock mass and the seismostratigraphy, confirm what was obtained from the geotechnical surveys, revealing the presence of two distinct seismostrata; the first is characterised by thicknesses between 2 and 5 m, and the second has thicknesses of around 19–20 m, characterised by velocities increasing with depth. There is further agreement between the surface investigations in that the refraction seismic section and the MASW seismostratigraphy provide comparable thicknesses for the first layer, which has slower Vp and Vs than the layer under test (Figure 8A,B). The MASW test detects the presence of a third seismic layer, characterised by Vs above 700 m/s, which, as assumed from the HVSR test, could have thicknesses of 45–60 m. The geomechanical survey did not

affect this seismostratum, probably corresponding to an even thicker tuffaceous lithotype. The data thus obtained made it possible to apply certain methods for evaluating the stability of cavities. In particular, empirical, simplified, and computed calculation methods were used. Carter's empirical method provided a picture of substantial stability, indicating possible instabilities only for the rooms of cavity two housed in the lowest quality cluster. In addition, it points to a possible boundary situation in room 1 of cavity 2. This may be attributable to the room size, which reaches borderline situations precisely for geometric reasons. The rooms in the other cavities are smaller and comparable in size. Hence, it is conceivable, as we do not yet have the complete mapping of the cavities in Grotte di Castro, that the more-or-less standardised dimensions of the rooms are a sort of adaptation, discovered over time, following the collapse of larger cavities. Harp and Noble's method still emphasises the difference between the qualities of the rock mass, indicating a decreasing value of Q" in the same degree as the quality of the rock mass. However, it detects an average susceptibility to collapse in an earthquake. It should be emphasised that the method assesses the susceptibility of collapse with a seismic event of magnitude 5. Given the seismic hazard maps of Grotte di Castro and the magnitude/distance disaggregation analysis for an event with a return time of 475 years, events with magnitude 5.5 and 6 are expected in the area within 20 km, although with much lower probability than an event with M = 5. Comparable results were obtained from the simplified calculation method but applied only to the rooms, not the connecting corridors. This choice was made because the safety factors for these structures were extremely conservative, perhaps due to their particular geometry. This method also highlights the poor condition of the central and terminal part of cavity 2. As shown in Figure 11, this cavity required some structural interventions over time, well represented by constructing masonry buttresses. From a quick diamine of the mortar used, it has been estimated that these structures were erected between the late 1800s and early 1900s (Figure 11B). Given the length of this cavity, it was possible to assume it was an ancient quarry. As the cavity progresses and encounters the less qualitative part of the mass, one notices a gradual downsizing of the rooms that, judging by the collapses (Figure 11A,C) and the results of the methods, is insufficient to maintain static stability. The Examine^{2D} software provided perhaps the best vantage point for assessing stability, finding areas of potential instability in all the cavities. However, except for the sections mentioned in cavity 2, these areas are very small and probably attributable to the fractures present. These areas tend to double in size when considering the accelerations of an earthquake (at least according to the preliminary methods used in this study), amplified by the local context, reaching values that are no longer negligible.

The picture that emerges from a static point of view and in the cavities examined is one of fundamental stability with some local situations, found in several rooms and corridors, especially in the more superficial cavities, that may induce instability. As can be seen from Figure 12, the cracking framework of some rooms, in particular, can generate risky situations. It can be seen that there are numerous highly open fractures and the presence of wedges, albeit small in size, already mobilised along the joints of the vault (Figure 12A–C). In addition, as the measurements were carried out following meteorological events, slight water ingress was noted on the vault and along the joints (Figure 12D). According to the meteorological data examined, 95 rainy days per year are recorded in this particular area of the municipality of Grotte di Castro. The percolation movements observed in the cavities, especially the more superficial ones, may change the current resistive parameters of the mass, evolving towards local situations of instability.



Figure 11. Images of cavity 2, collapse on the vault (**A**), masonry buttresses (**B**), and collapsed material on the floor (**C**).

As a result of the above, it is possible to consider using multiple methodologies to assess the stability of cavities. From what we have seen, empirical methodologies provide general indications for delineating areas of the cavities that could manifest criticalities, as do, similarly, simplified calculation methodologies. These methodologies, designed for problems related to mining excavations, may be challenging to adapt to the context of man-made cavities in soft rock, and must therefore be carefully selected and evaluated when framing the problem. An example to be considered comes from the graphical stability method [58], according to which the hydraulic radius of the cavities is compared with the stability number N, which is a function of the properties of the rock mass, the loads and the orientation of the stope/joints. This method has been widely used and is, with merit, recognised as a reliable methodology. Applied to the surveyed cavities, this method would be somewhat misleading in that only because of the hydraulic radius would all the surveyed cavities fall within the stable zone, even when estimating the number N with extreme caution (Figure 13). So, for many of the halls in the corridors considered, it would provide a true result comparable with the other methods. Still, it would also give us stability in the halls and corridors in cavity two's final part, showing tangible unstable conditions.

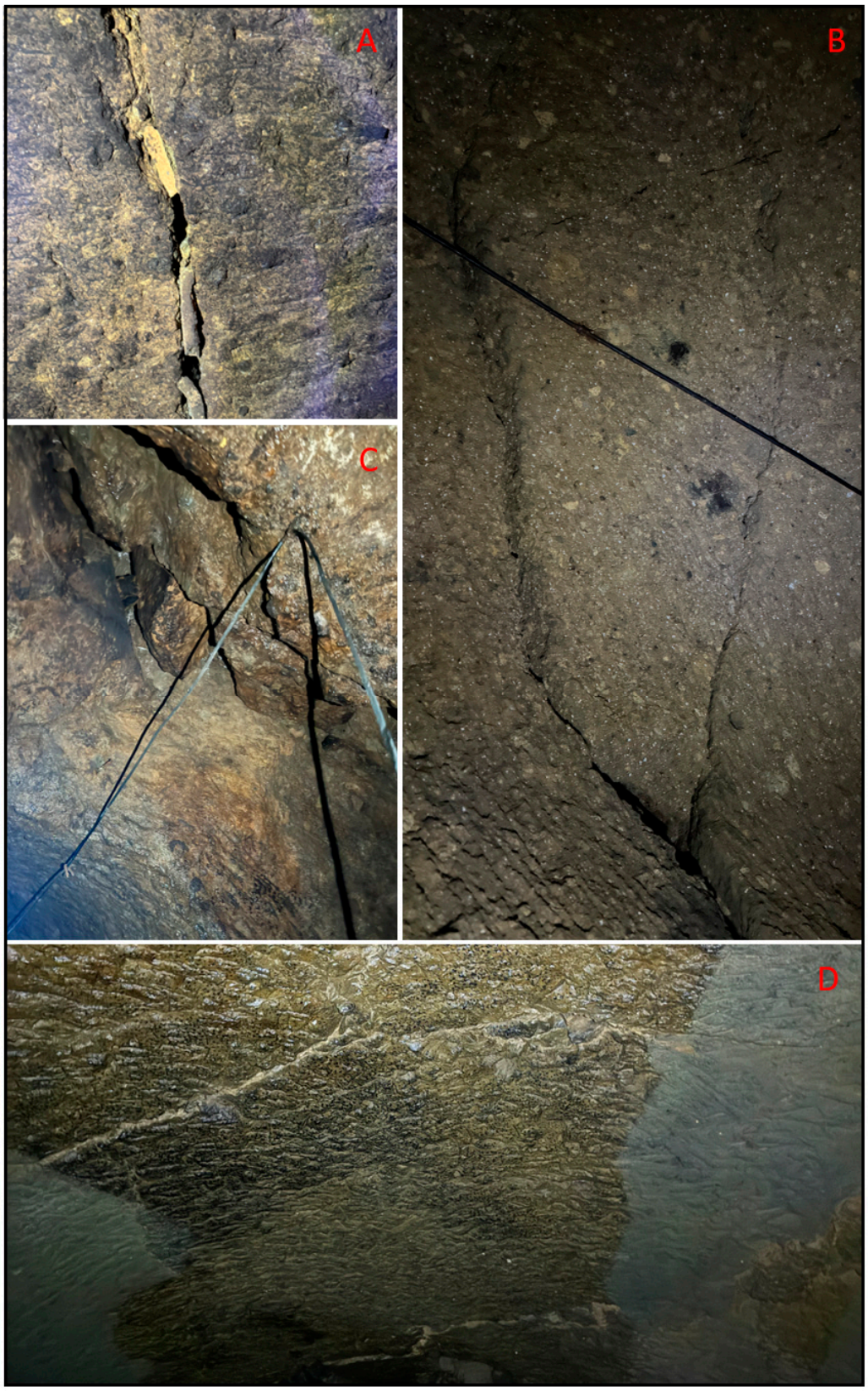


Figure 12. Open fracture (note the anthropogenic plugging on the inside) (**A**), fractures on the vault of one (**B**), small mobilised wedge (note the edges wetted by percolation water) (**C**), moisture and modest water ingress on the vault (**D**).

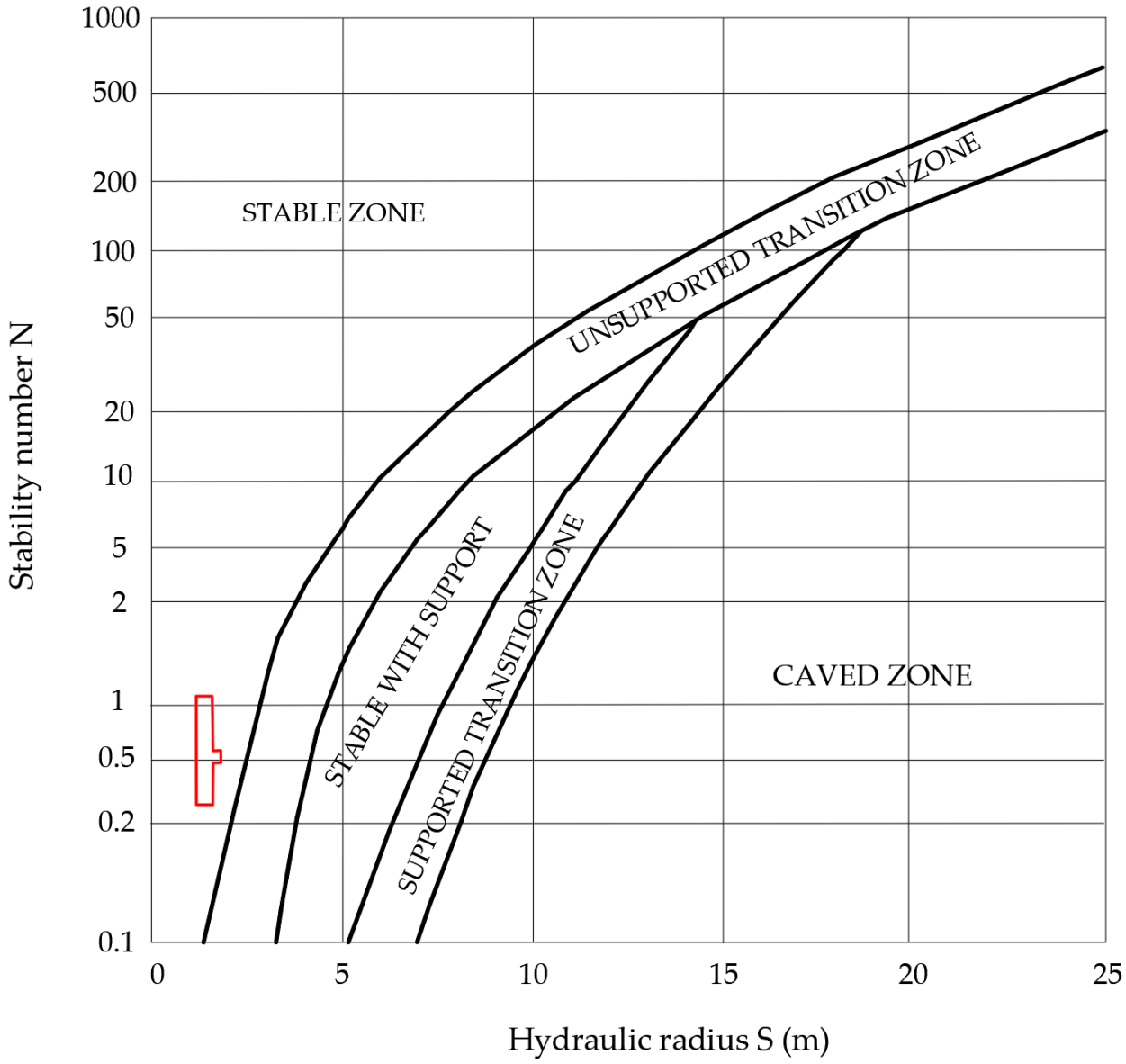


Figure 13. Stability graph. Assuming very conservative N values, all cavities fall within the red polygon.

However, other methodologies developed for the same problems in soft rock are highly specific, such as that of Bernabini [59,60] based on the calculation of the Cracking Degree. The relationship that allowed this parameter to be evaluated was valid for the red pozzolans of Rome, so we still do not know whether it applies to vulsine ignimbrites. Ultimately, noting that some portions of the cavities were close to the surface and that due to the seismic simulations the collapse volumes involved could also affect the ground level, a local reconstruction of the susceptibility to anthropogenic sinkholes was attempted for this area. Starting from the simulations conducted with Examine^{2D} from a seismic point of view, areas were identified where sinkholes are given as permissible over significant areas with a factor of safety < 1 and at a maximum of 5 m above ground level. In addition, areas where sinkholes are likely to occur were also indicated, with safety factors ranging from about 1 to 1.3. Areas with more-or-less pronounced deformations around the cavities were also indicated. The result, contemplated for the five cavities plus the two detected in 2024 [9] (for which no detailed simulations were carried out), is shown in Figure 14.

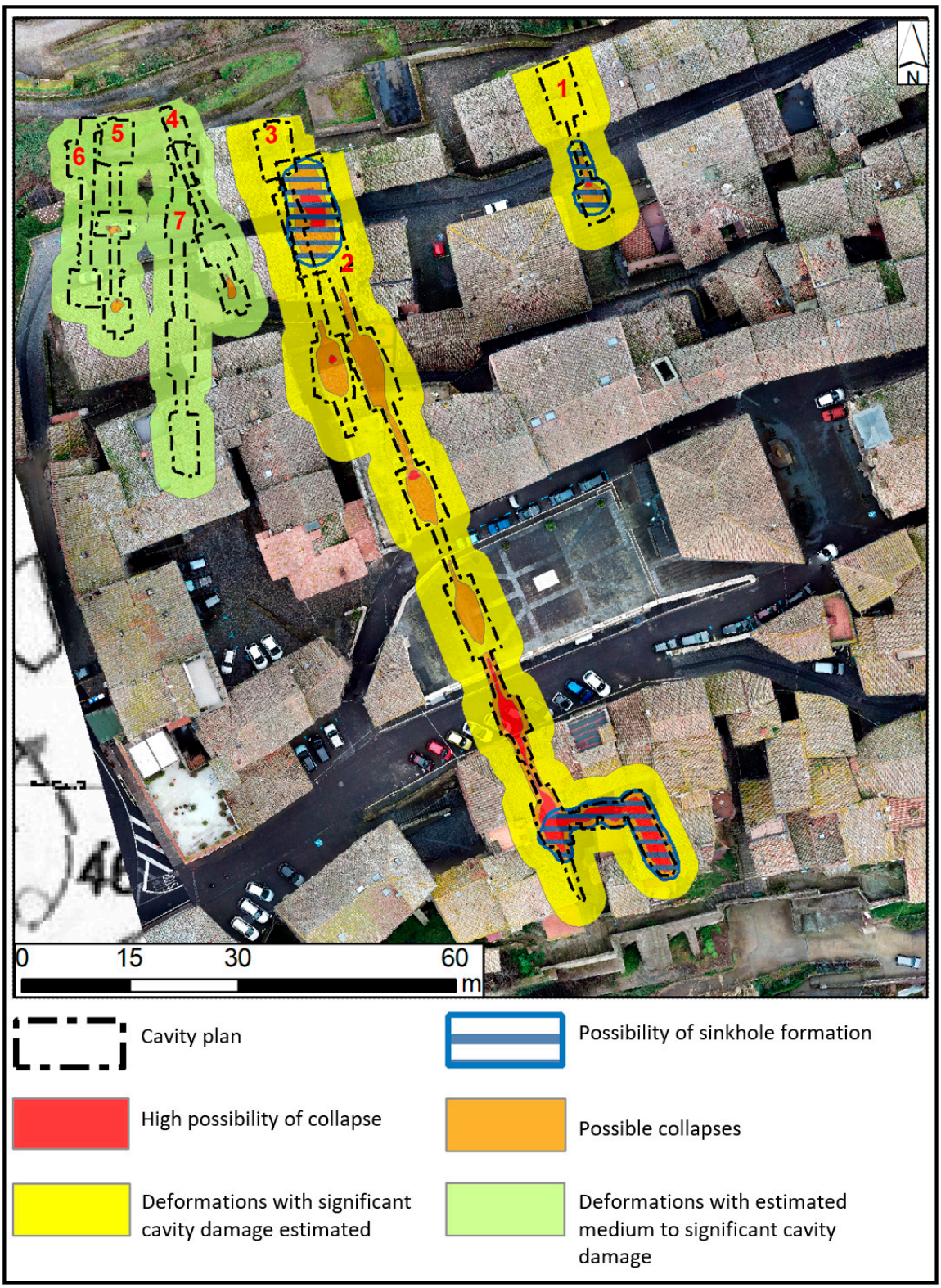


Figure 14. Attempt to construct anthropogenic sinkhole susceptibility map. The numbers 6 and 7 indicate the cavities detected in 2024 [9].

Based on the experience gathered during the experimentation in the municipality of Grotte di Castro, a method was developed, schematised in Figure 15, which summarises the path followed and makes what is reported in this article easily reproducible in other contexts.

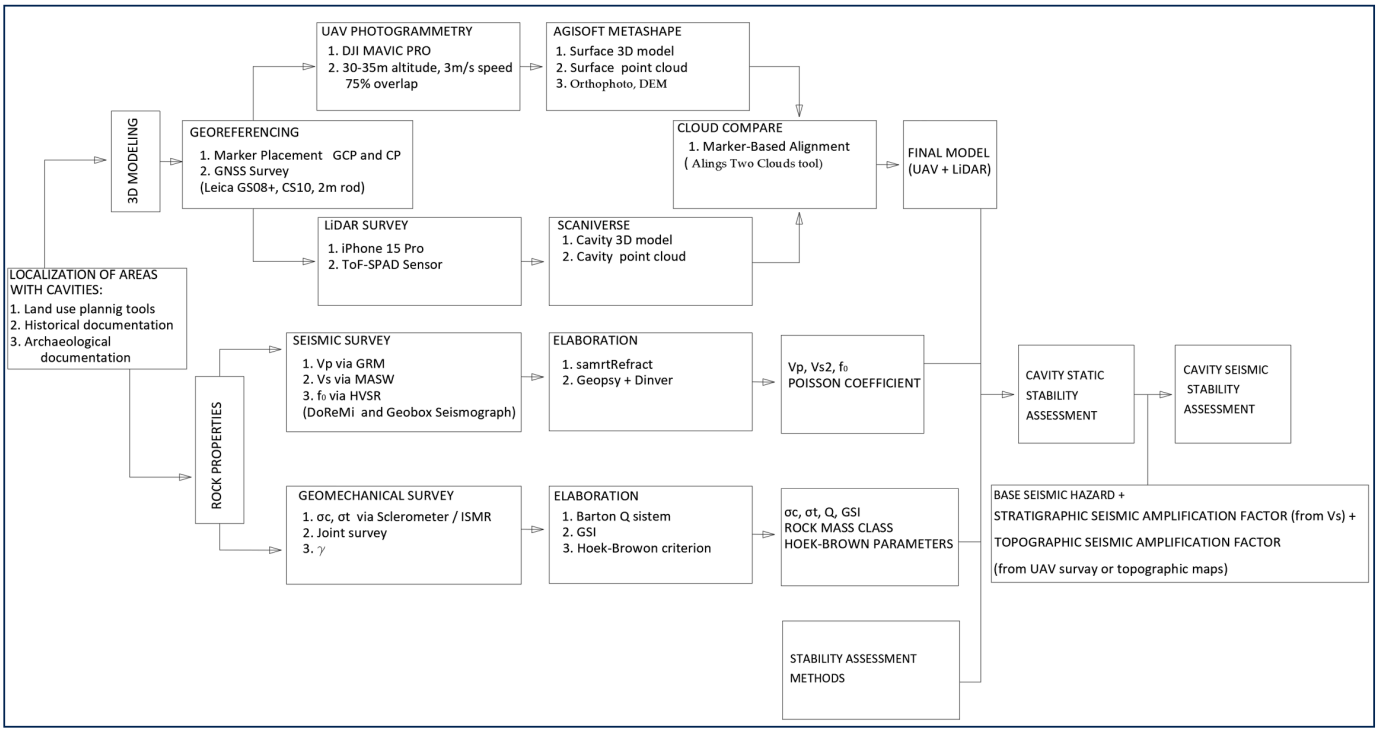


Figure 15. Activity flowchart.

6. Conclusions

It is clear from this work that any possibility of assessing certain geological hazards, such as seismic and sinkhole hazards, is essentially useless without knowing, at least indicatively, the position of underground cavities and their relationship to the surface. In geotechnical modelling and assessing the stability of these structures, the methods to be employed must be carefully considered, regardless of the level of knowledge to be achieved. It is therefore advisable to employ several methods and to compare the various results with each other to understand whether one has arrived at reliable results. For the town of Grotte di Castro, these censuses should continue to improve the knowledge acquired in this study, as the presence of other cavities and their spatial arrangement in relation not only to the surface but also to other underground structures can also significantly alter what has been deduced to date. Hence, it is important to develop census techniques and 3D modelling for these ancient excavations. A well-conducted census, in addition to contributing significantly to mitigating geological risk, is also the first step towards enhancing the value of these cavities, public enjoyment, safeguarding these assets, and reintegrating them into the fabric of the city, as has been achieved in other Italian cities (and elsewhere) by including underground cavities among their attractions.

Author Contributions: Conceptualisation, F.G., S.M. and S.N.; methodology, F.G.; software, F.G.; validation, F.G., S.M. and S.N. Formal analysis, F.G.; investigation, F.G.; resources, F.G.; data curation, F.G.; writing—original draft preparation, F.G.; writing—review and editing, S.M. and S.N.; visualisation, F.G.; supervision, S.M.; project administration, S.N.; funding acquisition, S.N. All authors have read and agreed to the published version of the manuscript.

Funding: This research was partially funded by PNRR—European Union—NextGenerationEU—Mission 4 "Education and Research"—Component 2 "From Research to Business"—Investment 3.1 "Fund for the realisation of an integrated system of research and innovation infrastructures". CUP: I53C22000800006.

Data Availability Statement: The datasets presented in this article are not readily available because the data are part of an ongoing study. Requests to access the datasets should be directed to francesco.gentili@unitus.it.

Conflicts of Interest: The authors declare no conflicts of interest.

References

1. Ministero delle Infrastrutture e dei Trasporti. Norme Tecniche per le Costruzioni (NTC 18). Decreto Ministeriale 17 Gennaio 2018. Available online: https://www.mit.gov.it/ (accessed on 15 February 2025).
2. *Fairbridge (1968)—The Encyclopedia of Geomorphology*; Reinhold: New York, NY, USA, 1968; p. 1295.
3. Nisio, S. The sinkholes: Teminological problmes, genetic mechanism, classification. *Mem. Descr. Carta Geol. D'it.* **2008**, *85*, 17–32.
4. Bonamini, M.; Di Maggio, C.; Lollino, P.; Madonia, G.; Parise, M.; Vattano, M. Sprofondamenti di origine antropica nell'area di Marsala (Sicilia occidentale) analizzati mediante rilievi in sito e analisi numerica dei processi di instabilità nelle cave sotterranee. *Mem. Descr. Carta Geol. D'italia* **2013**, *93*, 105–120.
5. Parise, M.; De Pascalis, A.; De Pascalis, F.; Donno, G.; Inguscio, S. Cavita sotterranee a fini estrattivi, e loro connessione con fenomeni di sprofondamento e subsidenza in agro di Cutrofiano (Lecce). *Atti Spelaion 2006 Borgo San Celano FG* **2008**, 55–69.
6. Madonna, S.; Nisio, S.; Finocchiaro, G.; Gentili, F. Le cavità antropiche presenti nel sottosuolo di Bolsena. *Mem. Descr. Carta Geol. D'it.* **2020**, *107*, 383–396.
7. Madonna, S.; Nisio, S.; Vessella, F. Primo contributo al censimento delle cavità sotterranee di Viterbo. *Mem. Descr. Carta Geol. D'it.* **2021**, *108*, 339–352.
8. Madonna, S.; Gentili, F.; Mattioli, M.; Scatolini, A.; Pendola, V.; Monaldi, G.G.; Monaldi, G. Survey techniques integrating smartphone LiDAR and UAV photogrammetry: The example of the anthropic underground cavities of Montefiascone (Viterbo, Central Italy). *Rend. Online Soc. Geol. It.* **2024**, *64*, 26–34. [CrossRef]
9. Gentili, F.; Madonna, S. Photogrammetry from UAV and Low-Cost LiDAR for Sinkhole Hazard Mitigation in Urban Areas: Applications and Evaluations. *Geographies* **2024**, *4*, 343–362. [CrossRef]
10. Sapia, V.; Materni, V.; Florindo, F.; Marchetti, M.; Gasparini, A.; Voltattorni, N.; Civico, R.; Giannattasio, F.; Miconi, L.; Marabottini, M.F.; et al. Imaging multiparametrico di tombe a camera etrusche: Caso di studio Grotte Di Castro (Italia). *Appl. Sci.* **2021**, *11*, 7875. [CrossRef]
11. Autorità di Bacino Distrettuale Appennino Centrale Piano di Assetto Idrogeologico Autorità di Bacino Distrettuale Appennino Centrale. Available online: https://aubac.it (accessed on 15 February 2025).
12. Washington, H.S. *The Roman Comagmatic Region*; Carnegie Institute Washington: Washington, DC, USA, 1906; Volume 36, pp. 1–220.
13. Locardi, E.; Lombardi, G.; Funiciello, R.; Parotto, M. The main volcanic groups of the Latium (Italy): Relations between structural evolution and petrogenesis. *Geol. Romana* **1976**, *16*, 279–300.
14. Sparks, R.S.J. Stratigraphie et géologie des ignimbrites du volcan Vulsini, Italie centrale. *Geol. Rundsch.* **1975**, *64*, 497–523. [CrossRef]
15. Nappi, G.; Renzulli, A.; Santi, A. Geological evolution and geochronology of the Vulsini volcanic district (central Italy). *Boll. Soc. Geol. Ital.* **1995**, *114*, 599–613.
16. Acocella, V.; Palladino, D.; Cioni, R.; Russo, P.; Simei, S. Caldera structure, amount of collapse, and erupted volumes: The case of Bolsena caldera, Italy. *Geol. Soc. Am. Bull.* **2012**, *124*, 1562–1576. [CrossRef]
17. Cifani, G.; Tamburini, P.; Della Giovompaola, I.; Ceccarelli, L. *La Civita di Grotte di Castro. Ricognizioni ed Indagini di Scavo*, 1st ed.; Edizioni Quasar Roma-Autori e Edizioni Quasar di Severino Tognon srl: Via Ajaccio 41-43, Roma, Italy, 2024; pp. 7–99.
18. Tamburini, P. La Civita di Grotte di Castro. Materiali inediti per uno studio dell'insediamento. In *Annali Facoltà di Lettere e Filologia dell'Università degli Studi di Perugia, XVIII*; Aracne: Paris, France, 1981; pp. 119–138.
19. Tamburini, P. La Civita di Grotte di Castro. Note e documenti su di un insedia mento del territorio volsiniese. In *Annali della Fondazione per il Museo «Claudio Faina» II*; Edizioni Quasar: Roma, Italy, 1985; pp. 182–206.
20. Timperi, A. Nuove acquisizioni dai territori di Bolsena e Grotte di Castro. In *Archeologia del Sottosuolo (atti del 1° Congresso Nazionale di Archeologia del Sottosuolo, Bolsena 2005)*; Basilico, R., Bavagnoli, Del Lungo, S., Padovan, G., Wilke, K.P., Eds.; Archaeopress: Oxford, UK, 2007; pp. 197–222.
21. Salamone, F. *La Civita di Grotte di Castro. Carta Archeologica*; Università la Sapienza: Roma, Italy, 2011; pp. 20–36.
22. Marabottini, M.F.; Tamburini, P. *Grotte di Castro: Il Territorio, il Paese, il Museo*; Sistema Museale del Lago di Bolsena: Quaderno, Italy, 2007; pp. 7–31.
23. Tamburini, P. Contributi per la storia del territorio volsiniese, I. I cippi funerari e l'onomastica. *MEFRA* **1987**, *99*, 635–659.
24. Fiumi, L. Codice diplomatico della Città di Orvieto. Firenze 1884. Available online: https://archive.org/details/codicediplomatic00fumiuoft (accessed on 1 January 2025).

25. Peel, M.C.; Finlayson, B.L.; McMahon, T.A. Updated world map of the Köppen-Geiger climate classification. *Hydrol. Earth Syst. Sci.* **2007**, *11*, 1633–1644. [CrossRef]
26. Colomina, I.; Molina, P. Unmanned aerial systems for photogrammetry and remote sensing: A review. *ISPRS J. Photogramm. Remote Sens.* **2014**, *92*, 79–97. [CrossRef]
27. Pingel, T.J.; Saavedra, A.; Cobo, L. Deriving Land and Water Surface Elevations in the Northeastern Yucatán Peninsula Using PPK GPS and UAV-Based Structure from Motion. *Pap. Appl. Geogr.* **2021**, *7*, 294–315. [CrossRef]
28. Puzzilli, L.; Ruscito, V.; Madonna, S.; Gentili, F.; Ruggiero, L.; Ciotoli, G.; Nisio, S. Natural sinkhole monitoring and characterization: The case of Latera sinkhole (Central Italy). *Geosciences* **2024**, *14*, 18. [CrossRef]
29. Agisoft LLC. Agisoft Metashape (Version 1.6.3) [Software]. 2020. Available online: https://www.agisoft.com (accessed on 16 July 2021).
30. Monsalve, A.; Yager, E.M.; Tonina, D. Evaluating Apple iPhone LiDAR measurements of topography and roughness elements in coarse bedded streams. *J. Ecohydraul.* **2023**, 1–11. [CrossRef]
31. King, F.; Kelly, R.; Fletcher, C.G. New opportunities for low-cost LiDAR-derived snow depth estimates from a consumer drone-mounted smartphone. *Cold Reg. Sci. Technol.* **2023**, *207*, 103757. [CrossRef]
32. Jerjomina, A.; Varbla, S. Advantages of low-cost LiDAR sensors in surveying underground utility networks. *Tunn. Undergr. Space Technol.* **2025**, *157*, 106325. [CrossRef]
33. Cloud Compare (Version 2.1) [GPL Software]. 2024. Available online: http://www.cloudcompare.org/ (accessed on 10 February 2025).
34. Gruppo di Lavoro. *Linee Guida per le Buone Pratiche dell'Analisi delle onde Superficiali*; CNR Edizioni: Rome, Italy, 2021; p. 135.
35. SESAME Team. *Guidelines for the Implementation of the H/V Spectral Ratio Technique on Ambient Vibrations: Measurements, Processing and Interpretation*; (Deliverable No. D23.12), WP12. 2004 SESAME European Research Project; European Commission: Brussels, Belgium, 2004.
36. Palmer, D.L. *The Generalized Reciprocal Method of Seismic Refraction Interpretation*; Society of Exploration Geophysicists: Tulsa, OK, USA, 1980. [CrossRef]
37. Park, C.B.; Miller, R.D.; Xia, J. Multichannel analysis of surface waves. *Geophysics* **1999**, *64*, 800–808.
38. Nakamura, Y. A Method for Dynamic Characteristics Estimation of Subsurface Using Microtremor on the Ground Surface. *Railw. Tech. Res. Inst. Q. Rep.* **1989**, *30*, 25–33.
39. Coco, G.; Corrao, M. *Geofisica Applicata*; Dario Flaccovio Editore: Palermo, Italy, 2008.
40. Barton, N.; Lien, R.; Lunde, J. Engineering classification of rock masses for the design of tunnel support. *Rock Mech.* **1974**, *6*, 188–236.
41. I.S.R.M. (International Society for Rock Mechanics). Basic geotechnical description of rock masses. *Int. Journ Rock Mech. Min. Sci. Geom. Abstr.* **1981**, *18*, 85–110.
42. I.S.R.M. (International Society for Rock Mechanics). *Rock Characterization, Testing and Monitoring*; Brown, E.T., Ed.; Pergamon Press: Oxford, UK, 1981; p. 211.
43. Hoek, E.; Brown, E.T. Empirical Strength Criterion for Rock Masses. *J. Geotech. Eng.* **1980**, *106*, 1013–1035.
44. Hoek, E.; Brown, E.T. The Hoek-Brown Failure Criterion—A 1988 Update. In Proceedings of the 15th Canadian Rock Mechanics Symposium, Toronto, ON, Canada, 3–4 October 1988; University of Toronto: Toronto, ON, Canada, 1988; pp. 31–38.
45. Hoek, E. Strength of rock and rock masses. *ISRM News J.* **1994**, *2*, 4–16.
46. Carter, T.G. A new approach to surfacecrown pillar design. In Proceedings of the 16th Canadian Rock Mechanics Symposium, Sudbury, ON, Canada, 16–19 June 1992; pp. 75–83.
47. Carter, T.G. *Guidelines for Use of the Scaled Span Method for Surface Crown Pillar Stability Assessment*; Ontario Ministry of Northern Development and Mines: Sudbury, ON, Canada, 2014; pp. 1–34.
48. Harp, E.L.; Noble, M.A. An Engineering Rock Classification to Evaluate Seismic Rock-Fall Susceptibility and its Application to the Wasatch Front. *Environ. Eng. Geosci.* **1993**, *30*, 293–319.
49. Diederichs, M.S.; Kaiser, P.K. Stability of large excavations in laminated hard rock masses: The voussoir analogue revisited. *Int. J. Rock Mech. Min. Sci.* **1999**, *36*, 97–117.
50. Diederichs, M.S.; Kaiser, P.K. Tensile strength and abutment relaxation as failure control mechanisms in underground excavations. *Int. J. Rock. Mech. Min. Sci.* **1999**, *36*, 69–96.
51. Barton, N.; Choubey, V. The shear strength of rock joints in theory and practice. *Rock Mech.* **1977**, *10*, 1–54. [CrossRef]
52. Stucchi, M.; Meletti, C.; Montaldo, V.; Crowley, H.; Calvi, G.M.; Boschi, E. Seismic Hazard Assessment (2003–2009) for the Italian Building Code. *Bull. Seismol. Soc. Am.* **2011**, *101*, 1885–1911. [CrossRef]
53. Available online: https://esse1-gis.mi.ingv.it/ (accessed on 23 February 2025).
54. Deliberazione Giunta Regionale del Lazio 17 giugno 2014 n363. *Approvazione delle "Linee Guida per la Pianificazione Comunale o Intercomunale di Emergenza in Materia di Protezione Civile"*; Bollettino Ufficiale della Regione Lazio n.52 del 1/07/2014; Regione Lazio: Rome, Italy, 2014.

55. Albarello, D.; Cesi, C.; Eulilli, V.; Guerrini, F.; Lunedei, E.; Paolucci, E.; Pileggi, D.; Puzzilli, L.M. The contribution of the ambient vibration prospecting in seismic microzoning: An example from the area damaged by the 26th April 2009 l'Aquila (Italy) earthquake. *Boll. Geofis. Teor. Appl.* **2010**, *52*, 513–538.
56. QGIS Development Team. QGIS Geographic Information System. Version 3.16. Open Source Geospatial Foundation Project. Available online: https://qgis.org (accessed on 10 January 2024).
57. Madonna, S.; Nisio, S.; Gentili, F.; Vessella, F.; Scardozzi, G.; Romagnoli, G.; Di Nezza, M.; Di Filippo, M.; Pelorosso, M.; Pagano, G. The role of historical-archaeological sources integrated into the GIS environment with geological and geophysical data in the mitigation of geological risks in some urban areas. *Rend. Online Soc. Geol. It.* **2023**, *61*, 50–57. [CrossRef]
58. Potvin, Y.; Milne, D. Empirical cable bolt support design. In *Rock Support in Mining and Underground Construction. In Proceedings of the 16th Canadian Rock Mechanics Symposium, Sudbury, ON, Canada, 16–19 June 1992*; Kaiser, P.K., McCreath, D.R., Eds.; Balkema: Rotterdam, The Netherlands, 1992.
59. Bernabini, M. Un esempio di applicazione dei metodi sismici allo studio del comportamento statico dei pilastri in sotterraneo. In Proceedings of the Symposium AMS, Cagliari, Italy, 26–29 July 1965.
60. Bernabini, M.; Esu, F.; MartinettiI, S.; Ribacchi, R. On the stability of the pillars in a underground quarry worked through soft pyroclastic rocks. In Proceedings of the 1st ISRM Congress, Lisbon, Portugal, 25 September–1 October 1966; pp. 285–291.

Disclaimer/Publisher's Note: The statements, opinions and data contained in all publications are solely those of the individual author(s) and contributor(s) and not of MDPI and/or the editor(s). MDPI and/or the editor(s) disclaim responsibility for any injury to people or property resulting from any ideas, methods, instructions or products referred to in the content.